Biochemistry and Biophysics Reports 36 (2023) 101567

Contents lists available at ScienceDirect

Biochemistry and Biophysics Reports

journal homepage: www.elsevier.com/locate/bbrep

Ischemia–Reperfusion accelerates neointimal hyperplasia via IL-1β-mediated pyroptosis after balloon injury in the rat carotid artery

Haijun Wei [a,h,1], Runyu Liu [a,i,1], Ming Zhao [g,1], Yarong Ma [f], Yanzheng He [a], Xiaolei Sun [a,b,c,d,e,*]

[a] Department of General Surgery (Vascular Surgery), The Affiliated Hospital of Southwest Medical University, Luzhou, 646000, China
[b] Department of Interventional Medicine, The Affiliated Hospital of Southwest Medical University, Luzhou, 646000, China
[c] Laboratory of Nucleic Acids in Medicine for National High-level Talents, Nucleic Acid Medicine of Luzhou Key Laboratory, Southwest Medical University, Luzhou, 646000, China
[d] Key Laboratory of Medical Electrophysiology, Ministry of Education & Medical Electrophysiological Key Laboratory of Sichuan Province, Collaborative Innovation Center for Prevention and Treatment of Cardiovascular Disease of Sichuan Province, Institute of Cardiovascular Research, Southwest Medical University, Luzhou, 646000, China
[e] Cardiovascular and Metabolic Diseases Key Laboratory of Sichuan, Luzhou, 646000, China
[f] Department of Ophthalmology, The Affiliated Hospital of Southwest Medical University, Luzhou, 646000, China
[g] Department of Gastroenterology, Clinical Medical College and the First Affiliated Hospital of Chengdu Medical College, Chengdu, Sichuan, 610500, China
[h] Department of Vascular Surgery, Hospital of Chengdu University of Traditional Chinese Medicine, Chengdu, 610000, China
[i] Department of Hepatobiliary Pancreatic Vascular Surgery, The Second Affiliated Hospital of Chengdu Medical College (China National Nuclear Corporation 416 Hospital), Chengdu, 610057, China

ARTICLE INFO

Keywords:
Neointimal hyperplasia
ischemia–reperfusion
IL-1β
Pyroptosis

ABSTRACT

Background: Ischemia–reperfusion (IR) is a pathological process that causes secondary damage to blood vessels. However, whether IR can further worsen neointima formation after balloon injury and the detailed mechanism are unclear.

Methods: An *in vivo* model of balloon injury to the rat carotid artery was established to study the effect of IR following balloon injury on neointima formation. Smooth muscle cells (SMCs) were isolated from rat aortas and exposed to hypoxia-reoxygenation to mimic the IR process *in vitro*. The *in vitro* cell model was used to investigate the mechanism of IR-mediated neointima formation after balloon injury, which was further confirmed in an *in vivo* rat model.

Results: IR aggravated neointima formation in the rat carotid artery 2 weeks after balloon injury compared with that observed in the absence of balloon injury ($P < 0.001$). Compared with that of normal SMCs in the rat carotid artery, the expression of IL-1β, a key proinflammatory cytokine associated with pyroptosis, was increased more than 3-fold in the IR-induced neointima ($P < 0.0001$) and contributed to the proliferation and migration of rat primary aortic SMCs ($P < 0.0001$). This process was alleviated by the antioxidant acetylcysteine (NAC), suggesting its partial dependence on intracellular ROS. In the rat model of IR following balloon injury in the carotid artery, the carotid artery that was locally transfected with AAV carrying sh-IL-1β or sh-caspase-1, which alleviated neointima formation, as indicated by a reduction in intima-media thickness in the rat carotid artery ($P < 0.0001$).

Conclusion: Our results suggested that IR could promote IL-1β production in SMCs in the carotid artery after balloon injury and aggravate neointimal hyperplasia, which was alleviated by silencing caspase-1/IL-1β signaling in SMCs in the carotid artery. These results suggest that IL-1β may be an effective target to combat IR-related neointima formation.

* Corresponding author. Department of General Surgery (Vascular Surgery), The Affiliated Hospital of Southwest Medical University, Luzhou, 646000, China.
E-mail address: sunxiaolei@swmu.edu.cn (X. Sun).
[1] These authors contributed equally to this study.

https://doi.org/10.1016/j.bbrep.2023.101567
Received 11 July 2023; Received in revised form 22 October 2023; Accepted 23 October 2023

1. Introduction

Occlusive atherosclerosis of the arteries, such as the coronary and carotid arteries, seriously threatens human health and results in substantial personal and societal healthcare burdens. Currently, percutaneous vascular interventions, including balloon angioplasty and stenting, are the conventional approaches to restore blood flow in blocked arteries. Ischemia–reperfusion injury (IRI) occurs after the restoration of the blood supply following a period of ischemia [1]. Inflammation is a critical pathological process associated with IRI that is involved in damage and local dysfunction in multiple organs and tissues, such as the myocardium, kidney, and brain [2,3].

Restenosis is a variation of the classic healing reaction after injury. The balloon and stent cause vascular injury and endothelial denudation, leading to vascular remodeling and initiating local thrombosis and inflammation. Frequent restenosis accelerates the proliferation and migration of vascular smooth muscle cells (VSMCs), thus leading to neointimal hyperplasia [4]. In response to vascular injury, cells such as macrophages [5], endothelial cells [6] and even VSMCs [7] are stimulated to produce IL-1β and induce the proliferation of VSMCs, leading to intimal hyperplasia [8]. As a crucial proinflammatory cytokine, IL-1β is the key mediator of pyroptosis, which is a mode of programmed cell death that is characterized by dependence on caspase-1 and gasdermin D (GSDMD) and the release of proinflammatory molecules, including IL-1β [9]. During typical inflammasome-induced pyroptotic death, GSDMD is hydrolytically cleaved by activated caspase-1 to release its N-terminal domain (GSDMD-N), which can punch holes in the cell membrane, allowing the release of IL-1β via unconventional protein secretion [10]. However, it is still unclear whether IR can induce pyroptosis in VSMCs and lead to neointima formation after vascular injury.

In the present study, we established a cell model of hypoxia-reoxygenation and a rat model of ischemia in the carotid artery prior to balloon dilation and demonstrated that IR accelerated neointimal hyperplasia via IL-1β-mediated pyroptosis in the rat carotid artery after balloon injury.

2. Materials and methods

2.1. Cell culture and treatments

Primary smooth muscle cells (SMCs) were isolated from rat aortas and cultured as previously reported [11]. Briefly, the aortas of 6-week-old male rats were removed, and the adventitia was excised. Then, each aorta was cut into 1 mm-long explants and cultured in DMEM containing 20 % fetal bovine serum, 100 U/mL penicillin and 100 μg/mL streptomycin. Cells from passages three to nine were immunostained with SMC markers SM22 and α-SMA, which showed more than 90 % positive cells, and these cells were used for the experiments. For the *in vitro* IR model, SMCs were cultured in a hypoxic cell incubator (1 % O_2 + 5 % CO_2 + 94 % N_2) without serum. Twelve hours later, the SMCs were transferred to a normal cell incubator (37 °C, 5 % CO_2) and maintained for 12 h. The cells were treated with belnacasan (VX-765, 50 μM, HY-13205, MedChemExpress), necrosulfonamide (NSA, 1 μM, abs814352, Absin) and acetylcysteine (NAC, 5 mM, HY-B0215, MedChemExpress).

2.2. Transfection of siRNA targeting IL-1β

When primary SMCs reached 40%–60 % confluence, they were transfected with siRNAs targeting IL-1β or a scramble control using Lipofectamine® RNAiMAX Transfection Reagent (RIBOBIO, China) according to the provided protocol. The interference efficiency was examined by qRT–PCR.

2.3. Carotid artery balloon injury with IR

Male SD rats (200–350 g) were provided by the Animal Experimental Center of Southwest Medical University and kept in a specific pathogen-free environment in the Key Laboratory of Medical Electrophysiology, Ministry of Education. The experimental protocol successfully passed the audit of the Ethics Committee (KY2019053). All procedures followed the NIH Guide for the Care and Use of Laboratory Animals (NIH Publications No. 8023, 8th edition, 2011). Eight-week-old male SD rats were anesthetized with 3–4% isoflurane to induce anesthesia and were maintained with 1–1.5 % isoflurane in a nitrous oxide/oxygen (2:1) mixture during surgery. In the ischemia–reperfusion carotid artery balloon injury (IR-CABI) group, after an incision was made in the skin of the neck, the left common carotid artery was fully exposed and clamped at both ends to maintain vascular ischemia for 2 h. Then, the balloon was placed into the common carotid artery, followed by balloon dilation at 1.5 atm for 30 s. Next, the balloon was removed, the external carotid artery was ligated, blood flow was restored, and the skin incision was closed. In contrast, the normal carotid artery balloon injury (CABI) group was only subjected to balloon injury. The right common carotid artery was used as a control. The artery was collected 24 h or 2 weeks after surgery. During artery collection, the rats were anesthetized with isoflurane as described previously and were euthanized by isoflurane (2 %) narcosis. Before the operation, the rats consumed approximately 3–7 g of food and 4–7 ml of water per day. After the operation, milk or 10 % sucrose was used to maintain physical recovery. Then, a normal diet was resumed.

2.4. Application of adeno-associated viruses (AAVs) in vivo

AAV was manufactured by Hanbio Biotechnology (Shanghai, China). After the left common carotid artery was exposed, matrix glue containing AAV carrying IL-1β- and caspase-1-specific shRNA (sh-IL-1: GCTAGTGTGTGATGTTCCCATTAGA sh-Caspase-1: CCAGGAAGAGATGGATACAATCAAA) was evenly applied around the carotid artery and allowed to stand for 20 min before the wound was closed. Three weeks after transfection, the rats were anesthetized with isoflurane and subjected to further treatments.

2.5. Ultrasonography of the rat carotid artery

A Vevo3100 ultrasound instrument with a probe frequency of 21 MHz was used to examine the bilateral common carotid arteries and evaluate the inner diameter of the vessels. Briefly, the ultrasonic probe was placed in the center of the vessels in a two-dimensional real-time state, and the optimal volume was adjusted to make the angle between the ultrasound beam and the direction of blood flow that was less than 60°. Several cardiac cycles were observed continuously to obtain a clear blood flow velocity spectrum curve, and then frozen images were captured. The blood flow velocity, wall thickness and inner diameter of the carotid artery were measured.

2.6. Histological and morphometric analysis of the carotid artery

The carotid artery was isolated 2 weeks after carotid balloon injury and fixed in 4 % paraformaldehyde (PFA), followed by embedding in optimal cutting temperature complex (OCT). Before being embedded, the carotid artery was sectioned at a thickness of 500 μm below the bifurcation. Hematoxylin-eosin (H&E) staining was used to distinguish the adventitia, media and intima in transverse sections of carotid arteries. Image-Pro Plus software was used for morphometric analysis. The inner membrane area was calculated by subtracting the lumen area from the internal elastic lamina area, and the media area was calculated by subtracting the internal elastic lamina area from the external elastic lamina area.

2.7. Immunofluorescence staining

Frozen sections of carotid arteries were immunostained for 24 h with

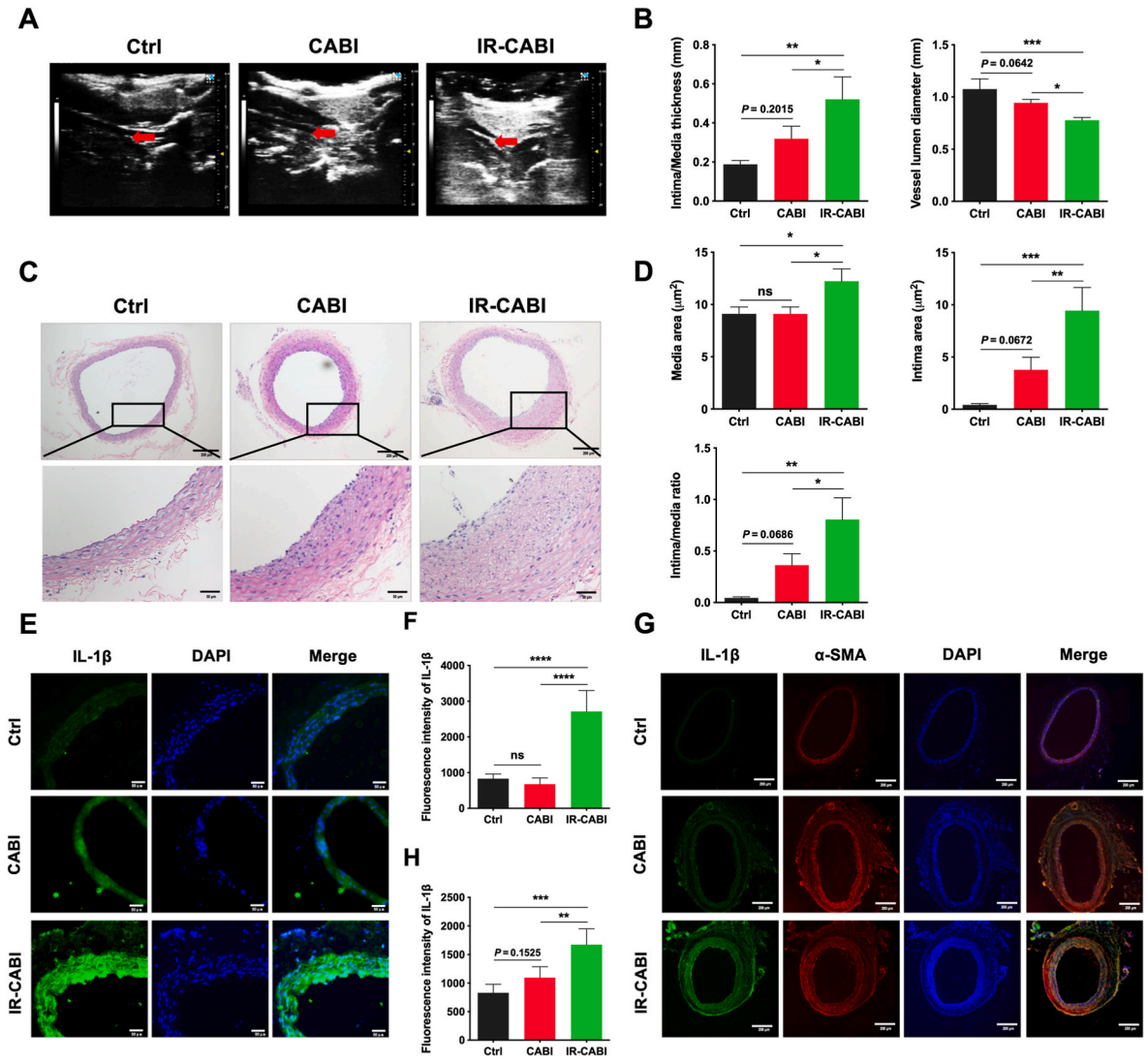

Fig. 1. IR aggravates neointima formation and increases IL-1β levels in the rat carotid artery wall after balloon injury. (A) Ultrasound examination of the thickness and inner diameter of the carotid artery, and the results are quantified in (B) ($n \geq 3$). (C) H&E staining showing the phenotype of neointima formation 2 weeks after carotid artery injury. (D) Quantification of the intima area, media area and ratio of intima to media area ($n \geq 3$). (E) Immunofluorescence staining of IL-1β 24 h after carotid artery injury. The fluorescence intensity of IL-1β was quantified in (F) ($n = 5$). (G) Co-immunofluorescence staining of IL-1β and α-SMA 2 weeks after carotid artery injury. The fluorescence intensity of IL-1β was quantified in (H) ($n = 6$). Ctrl, control group; CABI, normal carotid artery balloon injury group; IR-CABI, ischemia–reperfusion carotid artery balloon injury group. *P* values were determined by ANOVA with Tukey's multiple comparison test. $^{*}P < 0.05$, $^{**}P < 0.01$, $^{***}P < 0.001$, $^{****}P < 0.0001$, ns, not significant.

antibodies specific for SM-22 (ab14106; 1:100, rabbit, Abcam), α-smooth muscle actin (α-SMA) (ab7817; 1:100, mouse, Abcam), Caspase-1 (PA5-29342; 1:100, rabbit, Thermo Fisher Scientific), and IL-1β (ab300501; 1:50, rabbit, Abcam). After being extensively washed, the sections were incubated with secondary antibodies (Alexa 594 donkey anti-rabbit and Alexa 488 donkey anti-mouse IgGs (Invitrogen; 4 μg/mL) in PBST) for 1 h at room temperature and mounted with mounting medium containing DAPI (H-1200, Vector, Burlingame, CA). The slides were imaged using fluorescence microscopy (Till Polychrome V, Germany). Integrated optical density values were calculated using Image-Pro Plus software.

2.8. Cell counting kit (CCK)-8 assay

A cell counting kit (CCK-8 kit) (Solarbio, Beijing, China) was used to analyze cell proliferation. Primary rat aortic SMCs were treated with IR medium and seeded in a 96-well plate at a density of 1×10^4 cells per well. Twenty-four hours later, 10 μL of CCK-8 solution was added to 100 μL of cell culture medium. Wells containing culture medium and CCK-8 solution were used as blanks. After 2 h of incubation, the absorbance was measured at 450 nm with a microplate reader. Cell viability was determined with the following formula: Cell viability = [(ODIR-ODBlank)/(ODControl-ODBlank)] × 100 %. Cell proliferation was calculated by nonlinear regression using GraphPad Prism (version 5.0, La Jolla, CA).

2.9. Transwell migration assay

The transwell migration assay was performed using a chamber with 8 μm pores, which was immersed in a well containing 500 μL DMEM-F12 medium supplemented with 10 % FBS. Then, 1×10^4 cells in 100 μL of serum-free medium were plated into the upper chamber. Twelve hours later, the cells in the chamber were fixed with 4 % PFA and stained with crystal violet (KeyGENBioTECH, KGA229) for 20 min. A cotton swab was used to remove the cells in the upper chamber. The migrated cells in the lower surface of the chamber were imaged and quantified with

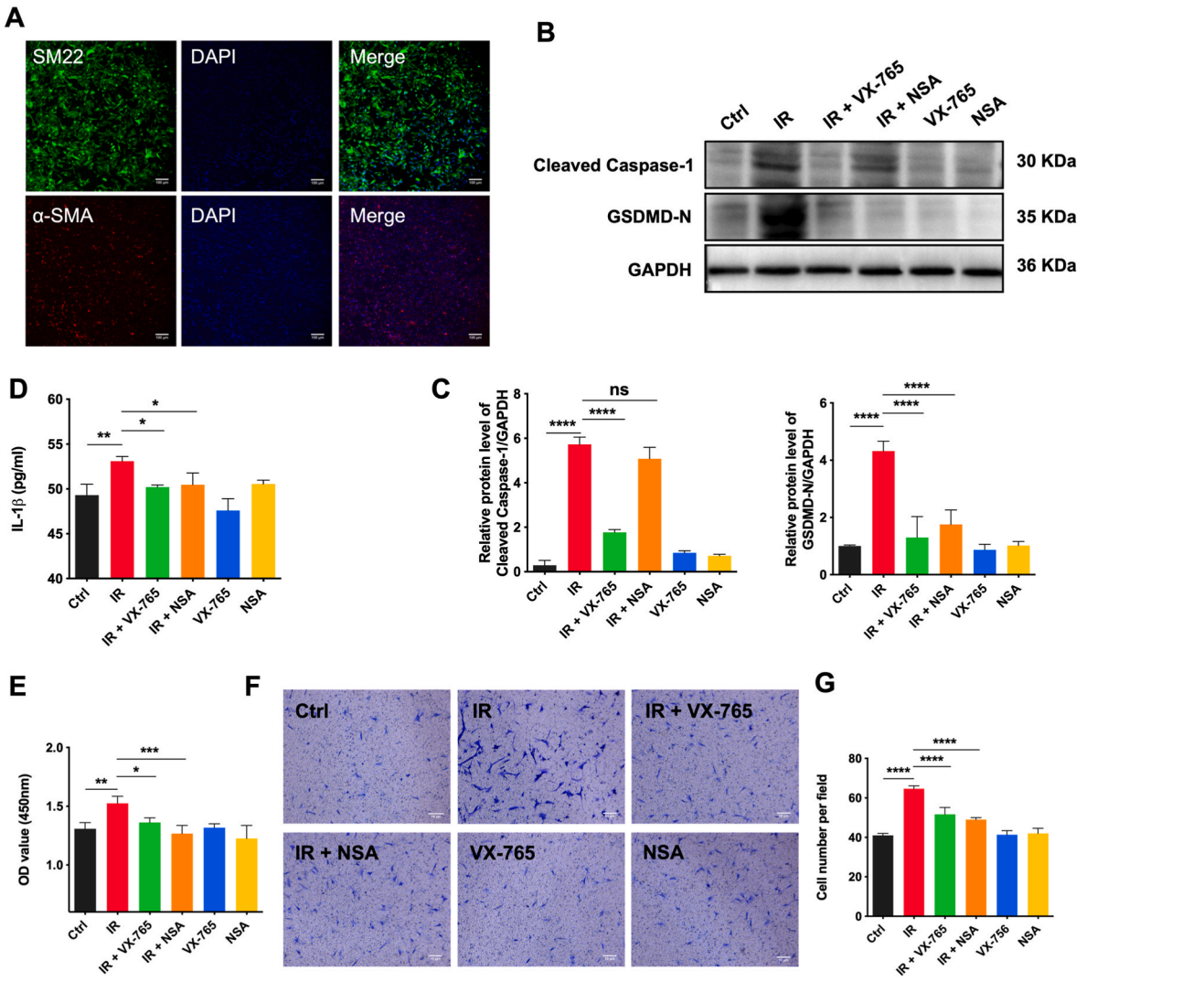

Fig. 2. IR-induced IL-1β secretion contributes to the proliferation and migration of rat primary aortic SMCs. (A) Immunostaining of primary rat SMCs for the markers SM22 and α-SMA. (B) Western blot analysis showing the protein levels of cleaved caspase-1 and GSDMD-N, and the results are quantified in (C) (n = 3). (D) ELISA showing the secretion of IL-1β into the culture medium (n = 3). (E) CCK-8 assay showing the growth of rat aortic SMCs (n = 4). (F) Transwell assay showing the migration of rat aortic SMCs, and the results are quantified in (G) (n = 3). VX-765, Caspase-1 inhibitor; NSA, GSDMD inhibitor. The concentrations of VX-765 and NSA were 50 μM and 1 μM, respectively. *P* values were determined by ANOVA with Tukey's multiple comparison test. $^{*}P < 0.05$, $^{**}P < 0.01$, $^{***}P < 0.001$, $^{****}P < 0.0001$.

Image-Pro Plus.

2.10. Wound healing assay

Primary rat aortic SMCs were seeded in a 6-well plate at 3×10^5 cells per well. When the cells reached 90 % confluence, they were scratched with a pipette tip in a straight line. The supernatant was replaced with medium with/without PDGF-BB (20 ng/mL). Twelve hours later, images were captured and the wound area was calculated.

2.11. Western blotting

Total proteins were extracted from cultured VSMCs or carotid arteries using lysis buffer supplemented with 1 % phosphatase inhibitor cocktail and 1 % phenylmethanesulfonyl fluoride (Beyotime Institute of Biotechnology). The proteins were separated by 10 % SDS–PAGE and transferred to polyvinylidene difluoride membranes (Millipore), which were blocked in 5 % nonfat milk for 60 min at room temperature. Then, the membranes were probed with antibodies against cleaved caspase-1 (#89332; 1:1000, rabbit, Cell Signaling Technology), GSDMD-N (#DF13758; 1:1000, rabbit, Affinity), and GAPDH (#2118; 1:10,000, rabbit, Cell Signaling Technology) at 4 °C overnight. An ECL substrate (Beyotime) was used to detect the signals with Universal-Hood II. To quantify protein levels, the density of the GAPDH and target protein bands was measured by ImageJ. GAPDH was used as a loading control. The relative protein levels were normalized to loading control levels (GAPDH).

2.12. Enzyme-linked immunosorbent assay (ELISA)

ELISA was used to detect the concentration of IL-1β. The supernatant of cultured SMCs subjected to hypoxia and reoxygenation was collected and frozen at −20 °C. Fifty microliters of supernatant was subjected to ELISA (JL18442, Jianglai Biological) according to the manufacturer's instructions.

2.13. Intracellular reactive oxygen species (ROS) evaluation

The intracellular ROS levels were measured by the cell-permeable probe DCFH-DA. SMCs were seeded in a 6-well plate at 1×10^5 cells per

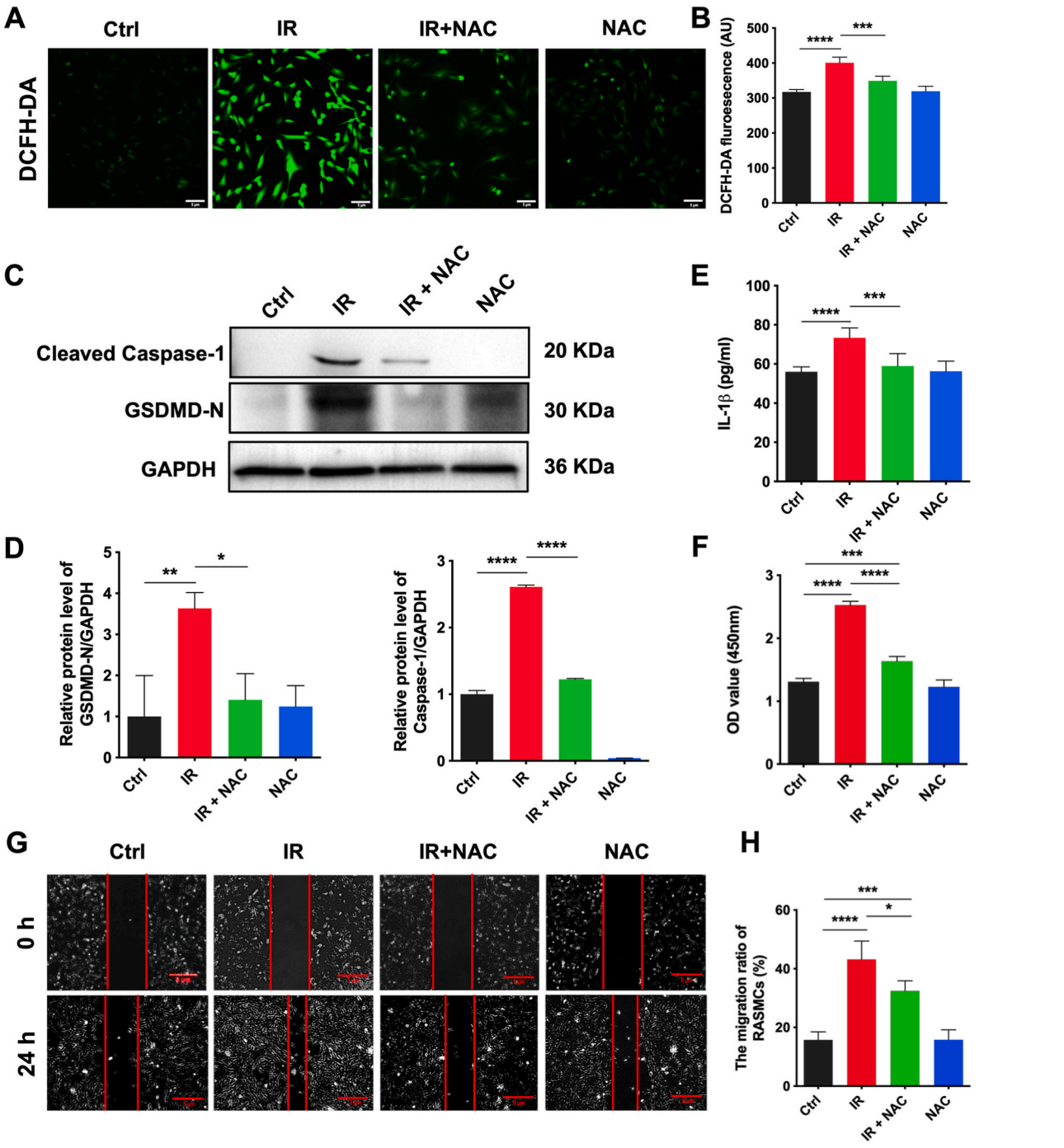

Fig. 3. ROS mediate IR-induced IL-1β expression and the proliferation and migration of rat aortic SMCs. (A) Representative images showing the DCFH-DA signals in SMCs. (B) Quantification of the DCFH-DA intensity in SMCs (n = 4). (C) Western blot analysis showing the protein levels of caspase-1 and GSDMD-N, and the results are quantified in (D) (n = 3). (E) ELISA showing the secretion of IL-1β into the culture medium (n = 6). (F) CCK-8 assay showing the growth of rat aortic SMCs (n = 4). (G) Transwell assay showing the migration of rat aortic SMCs, and the results are quantified in (H) (n = 4). NAC, ROS scavenger. The concentration of NAC was 5 mM. *P* values were determined by ANOVA with Tukey's multiple comparison test. $^{*}P < 0.05$, $^{**}P < 0.01$, $^{***}P < 0.001$, $^{****}P < 0.0001$.

well. The cells were treated with 500 μM NAC for 4 h and then subjected to the IR model *in vitro* for 24 h. After 3 washes with PBS, SMCs were treated with DCFH-DA (10 μM, S0033S, Beyotime Institute of Biotechnology, Beijing, China) at 37 °C for 20 min. The images were visualized by an Olympus FV3000 confocal microscope. The total fluorescence intensity of DCFH-DA and cell numbers were analyzed using ImageJ software, and the average fluorescence intensity of each cell was the value of total fluorescence intensity divided by the number of cells.

2.14. RNA purification and quantitative real-time PCR (qRT–PCR)

Total RNA was extracted from cells using TRIzol® reagent (Invitrogen) according to the provided protocol. cDNA was synthesized using the Transcriptor First Strand cDNA Synthesis Kit (Roche) and was used as the template for amplification using SYBR Green PCR Master Mix (Applied Biosystems).

The primers used for qRT–PCR were as follows:

Il-1β: forward: 5′-CTTCCTTGTGCAAGTGTCTGA-3′,

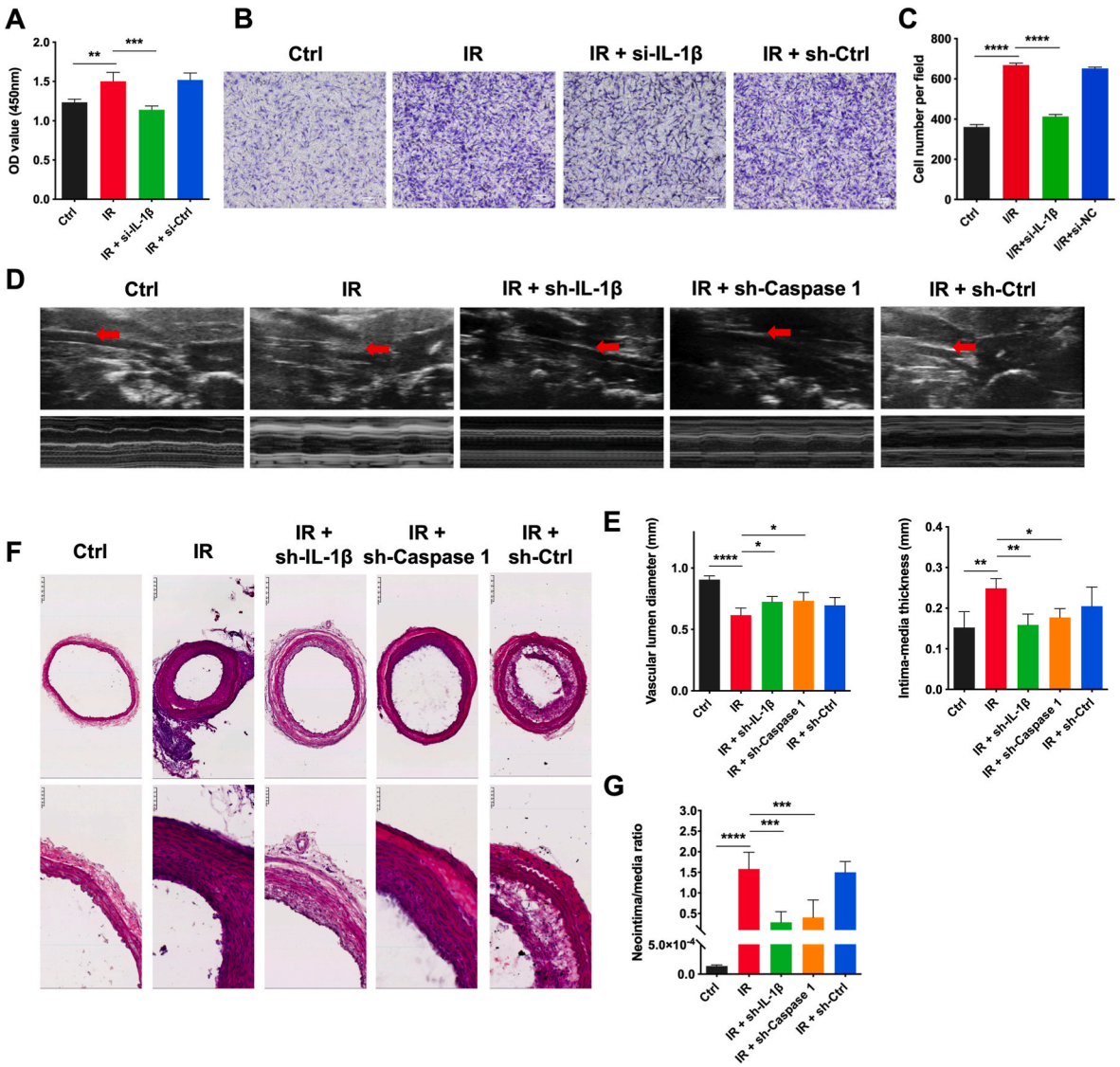

Fig. 4. Caspase-1/IL-1β signaling is essential for neointima formation in the rat carotid artery. (A) CCK-8 assay showing the growth of rat aortic SMCs (n = 4). (B) Transwell assay showing the migration of rat aortic SMCs, and the results are quantified in (C) (n = 4). (D) Ultrasound examination of the thickness and inner diameter of the carotid artery, which are quantified in (E) (n ≥ 3). (F) H&E staining shows the phenotype of neointima formation 2 weeks after carotid artery injury. (G) Quantification of the ratio of intima to media area (n ≥ 3). *P* values were determined by ANOVA with Tukey's multiple comparison test. $^{*}P < 0.05$, $^{**}P < 0.01$, $^{***}P < 0.001$, $^{****}P < 0.0001$.

reverse: 5′AGCCTCAAAGAACAGGTCATTCT-3';
GAPDH: forward: 5′-GGGTCCCAGCTTAGGTTCAT-3′,
reverse: 5′-GTTCACACCGACCTTACCACCA-3′).

mRNA levels were normalized to that of the endogenous gene GAPDH.

2.15. Statistical analysis

All data were analyzed using SPSS software (version 19.0, SPSS Inc., Chicago, IL, USA). Comparisons were analyzed by ANOVA with Tukey's multiple comparison test. Values are expressed as the means ± SDs, and $P < 0.05$ indicated statistical significance.

3. Results

3.1. IR enhances IL-1β expression in the neointima of the rat carotid artery

To test the hypothesis that IR can aggravate neointimal hyperplasia after carotid artery injury, we established a rat model with/without carotid ischemia for 2 h before balloon dilation (IR-CABI/CABI). Two weeks after surgery, ultrasound examination of the carotid artery revealed that rats with IR-CABI exhibited increased vessel wall thickness but a narrowed vessel lumen compared with control rats (Fig. 1A and B). Histologically, H&E staining of frozen sections confirmed this phenotype. Compared with those of control rats, the intima area, media area and ratio of intima to media area of IR-CABI rats were significantly increased (Fig. 1C and D). IL-1β is a key cytokine that can be secreted by SMCs and is involved in neointimal hyperplasia. We evaluated its expression in the carotid artery with/without CABI or IR-CABI by immunofluorescence analysis. IL-1β levels peaked 24 h after intervention in a rat model of focal cerebral ischemia [12], and the most severe degree of neointima regeneration occurred on days 14–28 [13]. Therefore, 24 h and 2 weeks were selected as short-term or long-term, respectively, to study IL-1β levels. Although IL-1β levels were not changed 24 h or 2 weeks after CABI, it was increased in IR-CABI rats (Fig. 1E–H). Notably, IL-1β colocalized with α-SMA, which is a marker of SMCs, suggesting that it was produced by SMCs (Fig. 1G). Taken

together, these results indicate that IL-1β expression is enhanced in the neointima of rats subjected to IR after carotid balloon injury, suggesting that IL-1β may be involved in the pathological process of neointima formation.

3.2. IR-related IL-1β secretion contributes to the proliferation and migration of rat primary aortic SMCs

To investigate whether IL-1β is derived from pyroptosis in SMCs, isolated primary aortic SMCs were exposed to hypoxia-reoxygenation to mimic the IR process. The markers SM22 and α-SMA were used to verify the high purity of SMCs (Fig. 2A). Based on this model, the cells exposed to hypoxia-reoxygenation were further treated with VX-765 or NSA to inhibit the expression of caspase-1 or gasdermin D (GSDMD), respectively, which are key molecules for pyroptosis. The caspase-1 inhibitor VX-765 significantly reversed the IR-induced expression of caspase-1 and downstream GSDMD, while GSDMD inhibitor NSA only significantly reversed IR-induced expression of GSDMD (Fig. 2B and C). As expected, the release of IL-1β into the culture medium was increased by IR but was alleviated by inhibiting caspase-1 or GSDMD with VX-765 or NSA, respectively (Fig. 2D). To test whether pyroptosis-derived IL-1β was involved in the proliferation and migration of rat aortic SMCs, a CCK-8 assay was performed, and the results showed that VX-765 and NSA alleviated IR-induced cell proliferation (Fig. 2E). Similarly, a transwell assay was used to examine the ability of VX-765 or NSA to alleviate IR-induced cell migration (Fig. 2F and G). Taken together, these results revealed that IL-1β was derived from pyroptotic SMCs exposed to hypoxia/reoxygenation, and the increase in IL-1β levels may be at least partially responsible for the increase in the proliferation and migration of SMCs.

3.3. IR-related IL-1β production is partially attributed to intracellular ROS

IR has been reported to induce the production of ROS [14], which are involved in pyroptosis [15]. To test whether ROS are mediators of IR-related IL-1β secretion during SMC pyroptosis, the fluorescent probe DCFH-DA was used to label intracellular ROS. As expected, IR induced ROS production, and ROS were scavenged by NAC (Fig. 3A and B). Notably, the ROS scavenger NAC decreased the IR-induced protein expression of caspase-1, GSDMD and IL-1β (Fig. 3C). Additionally, the alleviation of IR-induced protein expression of cleaved caspase-1 and GSDMD and the secretion of IL-1β were confirmed by Western blotting (Fig. 3C and D) and ELISA (Fig. 3E), respectively. Furthermore, NAC treatment decreased IR-induced proliferation (Fig. 3F) and migration (Fig. 3G and H) in SMCs. These data suggest that IR-related IL-1β secretion is partially dependent on ROS and essential for the proliferation and migration of SMCs.

3.4. Caspase-1/IL-1β signaling is essential for neointima formation in the rat carotid artery

Although an *in vitro* cell model was used to investigate the mechanism of IR-mediated neointima formation after balloon injury, the phenomenon is actually hyperoxia because in the body, the partial pressure of oxygen is less than 21 %, which is atmospheric pressure [16]. Therefore, this finding should be further confirmed in an *in vivo* rat model. To further elucidate the role of caspase-1/IL-1β signaling in IR-induced neointima formation in the rat carotid artery, an siRNA targeting IL-1β was used to specifically knock down IL-1β transcription (Fig. S1), and the results showed that si-IL-1β reversed IR-induced cell proliferation (Fig. 4A) and migration (Fig. 4B, C). We next investigated the role of caspase-1/IL-1β signaling in intimal hyperplasia after balloon injury. Rat carotid arteries were locally transfected with AAVs carrying sh-IL-1β or sh-caspase-1, which significantly reduced the protein levels of IL-1β and caspase-1 (Figs. S2A and B). Carotid ultrasound showed that IR increased the intima-media thickness of the carotid artery, and this effect was reversed by sh-IL-1β or sh-caspase-1 (Fig. 4D and E). Furthermore, this finding was confirmed by H&E staining 2 weeks postinjury (Fig. 4F, G). Taken together, these data indicate that caspase-1/IL-1β signaling is essential for neointima formation in the rat carotid artery.

4. Discussion

IR is a pathophysiological process that leads to organ and tissue dysfunction [17]. Blood supply restoration after long-term myocardial ischemia causes secondary damage to the myocardium [18]. Similarly, in the central nervous system, IR damages central neurons [19]. We also observed lower limb swelling after the recanalization of blood vessels via endovascular treatment in limbs exposed to long-term ischemia in clinical studies.

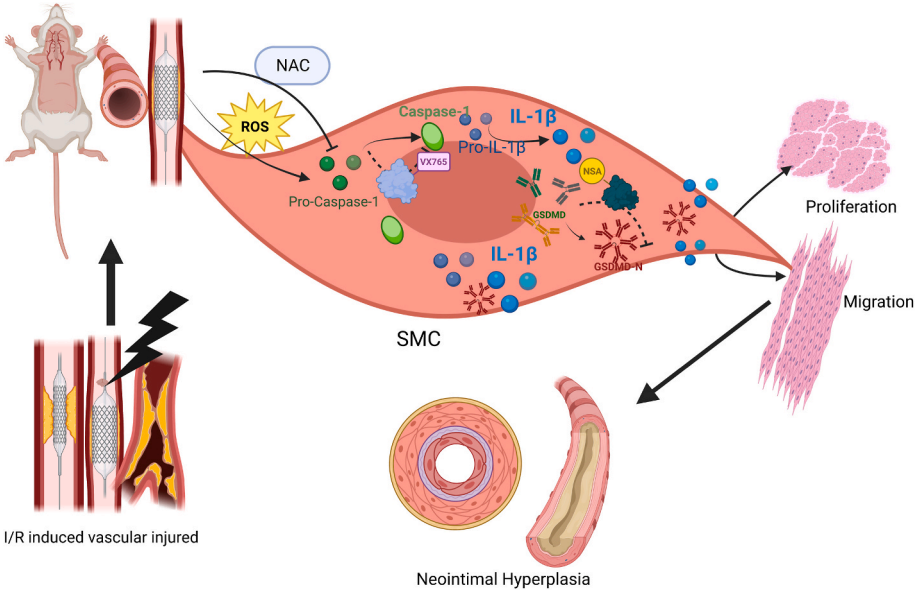

Fig. 5. Ischemia–Reperfusion accelerates neointimal hyperplasia via IL-1β-mediated pyroptosis after balloon injury in the rat carotid artery.

Physical injuries, such as balloon injury and stent implantation, have been reported to cause neointima formation [20]. However, the role of IR after vascular recanalization in neointima formation is still unclear. Ismaeel et al. showed that hypoxia-reoxygenation of cultured endothelial cells accelerated the secretion of the profibrotic factors platelet-derived growth factor (PDGF)-BB and connective tissue growth factor (CTGF) and induced TGF-β1 production in SMCs, thereby enhancing the proliferation and migration of SMCs [21]. This finding suggests a possible role of IR in neointima formation. However, after carotid artery balloon injury, only a few endothelial cells survived to affect SMCs [22], suggesting that IR may directly affect the proliferation and migration of SMCs. In this study, we found that IL-1β was highly expressed in the tunica media rather than only in the intima 24 h after IR balloon injury, suggesting that IL-1β may be involved in IR-induced intimal neogenesis.

IL-1β has been shown to play an important role in neointima formation after vascular injury. This factor can directly activate MMP-2 in SMCs and promote their proliferation and migration [23]. In addition, IL-1β was reported to interact with MMP-9 to delay reendothelialization and promote neointima formation [7,24]. In this study, we showed that a large amount of IL-1β was produced by SMCs after hypoxia-reoxygenation, and reducing IL-1β expression with an siRNA inhibited the proliferation and migration of SMCs. Kikuo et al. constructed a mouse model with IL-1 receptor antagonist deficiency (IL-1Ra−/−) and revealed that IL-1Ra deficiency promoted neointima formation after injury [25]. François et al. reported that injection of the IL-1β modulator gevokizumab could similarly reduce neointima formation after carotid artery injury [26]. In the present study, local transfection of an shRNA targeting IL-1β in the carotid artery attenuated intimal hyperplasia. Thus, targeting IL-1β may be an effective strategy to combat IR-related neointima formation.

Pyroptosis is a process associated with abundant IL-1β production, and SMC pyroptosis is one of the major causes of neointima formation [27,28]. In the present study, IR after balloon injury increased the expression of pyroptosis-related proteins, including cleaved caspase-1, GSDMD-N and IL-1β, in SMCs. Inhibiting caspase-1 and IL-1β inhibited neointima formation after carotid artery injury *in vivo*, which suggests that IR can activate the pyroptosis pathway. It was reported that ROS are essential for high glucose-induced pyroptosis [29]. Here, we determined that IR could induce ROS production in SMCs, and treatment with the ROS scavenger NAC reduced IR-related pyroptosis and therefore induced subsequent neointima formation. However, the precise location of ROS in the vascular wall after local intimal injury of the carotid artery is unclear. Additionally, the mechanism by which ROS induce pyroptosis in SMCs needs to be further elucidated.

In conclusion, we revealed that IR could promote IL-1β production in SMCs after carotid artery balloon injury and induce the proliferation and migration of SMCs, thus leading to neointimal hyperplasia. Inhibiting IL-1β *in vivo* alleviated neointimal hyperplasia, suggesting that IL-1β may be an effective target to combat IR-related neointima formation (Fig. 5).

Author contributions

XLS conceptualized, designed and funded the study and revised and edited the manuscript. MZ helped revise and edit the manuscript. HJW and RYL performed the primary experiments. YRM prepared the materials for the experiments. YZH and CXZ reviewed the manuscript. All the authors have read and approved the final version of the manuscript.

Funding

This study was supported by the International Science and Technology Innovation Cooperation Project of Sichuan Province (22GJHZ0278), the Sichuan Science and Technology Program (2022YFS0614), the Medical Research Project of Sichuan Province (S21020), the Science and Technology Strategic Cooperation Project of Luzhou Municipal People's Government and Southwest Medical University (2021LZXNYD-D10), and the Doctoral Research Initiation Program of the Affiliated Hospital of Southwest Medical University (19041).

Declaration of competing interest

The authors have no conflicts of interest to declare.

Data availability

Data will be made available on request.

Acknowledgments

None.

Appendix A. Supplementary data

Supplementary data to this article can be found online at https://doi.org/10.1016/j.bbrep.2023.101567.

References

[1] H. Wang, Z. Xi, L. Deng, Y. Pan, K. He, Q. Xia, Macrophage polarization and liver ischemia-reperfusion injury, Int. J. Med. Sci. 18 (2021) 1104–1113, https://doi.org/10.7150/ijms.52691.
[2] E. Gouda, F. Babiker, Gum Arabic protects the rat heart from ischemia/reperfusion injury through anti-inflammatory and antioxidant pathways, Sci. Rep. 12 (2022), 17235, https://doi.org/10.1038/s41598-022-22097-0.
[3] S. Ghafouri-Fard, H. Shoorei, Y. Poornajaf, B.M. Hussen, Y. Hajiesmaeili, A. Abak, M. Taheri, A. Eghbali, NLRP3: role in ischemia/reperfusion injuries, Front. Immunol. 13 (2022), 926895, https://doi.org/10.3389/fimmu.2022.926895.
[4] C. Gareri, S. De Rosa, C. Indolfi, MicroRNAs for restenosis and thrombosis after vascular injury, Circ. Res. 118 (2016) 1170–1184, https://doi.org/10.1161/circresaha.115.308237.
[5] J. Yao, X. Zhao, F. Tan, X. Cao, S. Guo, X. Li, Z. Huang, K. Diabakte, L. Wang, M. Liu, Z. Shen, B. Li, Z. Cao, S. Sheng, M. Lu, Y. Cao, H. Jin, Z. Zhang, Y. Tian, Early modulation of macrophage ROS-PPARγ-NF-κB signalling by sonodynamic therapy attenuates neointimal hyperplasia in rabbits, Sci. Rep. 10 (2020), 11638, https://doi.org/10.1038/s41598-020-68543-9.
[6] S. Koka, M. Xia, Y. Chen, O.M. Bhat, X. Yuan, K.M. Boini, P.L. Li, Endothelial NLRP3 inflammasome activation and arterial neointima formation associated with acid sphingomyelinase during hypercholesterolemia, Redox Biol. 13 (2017) 336–344, https://doi.org/10.1016/j.redox.2017.06.004.
[7] M.E. Mantione, M. Lombardi, D. Baccellieri, D. Ferrara, R. Castellano, R. Chiesa, O. Alfieri, C. Foglieni, IL-1β/MMP9 activation in primary human vascular smooth muscle-like cells: exploring the role of TNFα and P2X7, Int. J. Cardiol. 278 (2019) 202–209, https://doi.org/10.1016/j.ijcard.2018.12.047.
[8] G. Lopez-Castejon, D. Brough, Understanding the mechanism of IL-1beta secretion, Cytokine Growth Factor Rev. 22 (2011) 189–195, https://doi.org/10.1016/j.cytogfr.2011.10.001.
[9] P. Yu, X. Zhang, N. Liu, L. Tang, C. Peng, X. Chen, Pyroptosis: mechanisms and diseases, Signal Transduct. Targeted Ther. 6 (2021) 128, https://doi.org/10.1038/s41392-021-00507-5.
[10] L. Sun, W. Ma, W. Gao, Y. Xing, L. Chen, Z. Xia, Z. Zhang, Z. Dai, Propofol directly induces caspase-1-dependent macrophage pyroptosis through the NLRP3-ASC inflammasome, Cell Death Dis. 10 (2019) 542, https://doi.org/10.1038/s41419-019-1761-4.
[11] Q. Xiao, F. Zhang, G. Grassia, Y. Hu, Z. Zhang, Q. Xing, X. Yin, M. Maddaluno, B. Drung, B. Schmidt, P. Maffia, A. Ialenti, M. Mayr, Q. Xu, S. Ye, Matrix metalloproteinase-8 promotes vascular smooth muscle cell proliferation and neointima formation, Arterioscler. Thromb. Vasc. Biol. 34 (2014) 90–98, https://doi.org/10.1161/ATVBAHA.113.301418.
[12] K. Pan, Q. Peng, Z. Huang, Z. Dong, W. Lin, Y. Wang, Temporal patterns and distribution of pyroptosis-related molecules and effects of human mesenchymal stem cells on pyroptosis following cerebral ischemia/reperfusion in rats, J. Stroke Cerebrovasc. Dis. 32 (2023), 107199, https://doi.org/10.1016/j.jstrokecerebrovasdis.2023.107199.
[13] C.Y. Wong, M.R. de Vries, Y. Wang, J.R. van der Vorst, A.L. Vahrmeijer, A.J. van Zonneveld, P. Roy-Chaudhury, T.J. Rabelink, P.H. Quax, J.I. Rotmans, Vascular remodeling and intimal hyperplasia in a novel murine model of arteriovenous fistula failure, J. Vasc. Surg. 59 (2014) 192–201.e191, https://doi.org/10.1016/j.jvs.2013.02.242.
[14] J.F. Chang, H.L. Kuo, S.H. Liu, C.Y. Hsieh, C.P. Hsu, K.C. Hung, T.M. Wang, C. C. Wu, K.C. Lu, W.N. Lin, C.F. Hung, W.C. Ko, Translational medicine in uremic vascular calcification: scavenging ROS attenuates p-cresyl sulfate-activated caspase-1, NLRP3 inflammasome and eicosanoid inflammation in human arterial

smooth muscle cells, Life (Basel) 12 (2022), https://doi.org/10.3390/life12050769.
[15] R. Shen, P. Yin, H. Yao, L. Chen, X. Chang, H. Li, X. Hou, Punicalin ameliorates cell pyroptosis induced by LPS/ATP through suppression of ROS/NLRP3 pathway, J. Inflamm. Res. 14 (2021) 711–718, https://doi.org/10.2147/JIR.S299163.
[16] C. Zhou, Q.Y. Zou, Y.Z. Jiang, J. Zheng, Role of oxygen in fetoplacental endothelial responses: hypoxia, physiological normoxia, or hyperoxia? Am. J. Physiol.: Cell Physiol. 318 (2020) C943–c953, https://doi.org/10.1152/ajpcell.00528.2019.
[17] T. Zhao, W. Wu, L. Sui, Q. Huang, Y. Nan, J. Liu, K. Ai, Reactive oxygen species-based nanomaterials for the treatment of myocardial ischemia reperfusion injuries, Bioact. Mater. 7 (2022) 47–72, https://doi.org/10.1016/j.bioactmat.2021.06.006.
[18] C. Huang, S. Zhou, C. Chen, X. Wang, R. Ding, Y. Xu, Z. Cheng, Z. Ye, L. Sun, Z. J. Wang, D. Hu, X. Jia, G. Zhang, S. Gao, Biodegradable redox-responsive AIEgen-based-covalent organic framework nanocarriers for long-term treatment of myocardial ischemia/reperfusion injury, Small 18 (2022), e2205062, https://doi.org/10.1002/smll.202205062.
[19] Z. Fan, L. Cai, S. Wang, J. Wang, B. Chen, Baicalin prevents myocardial ischemia/reperfusion injury through inhibiting ACSL4 mediated ferroptosis, Front. Pharmacol. 12 (2021), 628988, https://doi.org/10.3389/fphar.2021.628988.
[20] T. Song, J. Zhao, T. Jiang, X. Jin, Y. Li, X. Liu, Formononetin protects against balloon injuryinduced neointima formation in rats by regulating proliferation and migration of vascular smooth muscle cells via the TGFbeta1/Smad3 signaling pathway, Int. J. Mol. Med. 42 (2018) 2155–2162, https://doi.org/10.3892/ijmm.2018.3784.
[21] A. Ismaeel, D. Miserlis, E. Papoutsi, G. Haynatzki, W.T. Bohannon, R.S. Smith, J. L. Eidson, G.P. Casale, Pipinos II, P. Koutakis, Endothelial cell-derived pro-fibrotic factors increase TGF-β1 expression by smooth muscle cells in response to cycles of hypoxia-hyperoxia, Biochimica et biophysica acta, Molecul. Basis Dis. 1868 (2022), 166278, https://doi.org/10.1016/j.bbadis.2021.166278.
[22] J. Kong, F. Wang, J. Zhang, Y. Cui, L. Pan, W. Zhang, J. Wen, P. Liu, Exosomes of endothelial progenitor cells inhibit neointima formation after carotid artery injury, J. Surg. Res. 232 (2018) 398–407, https://doi.org/10.1016/j.jss.2018.06.066.
[23] Z. Wang, L. Kong, J. Kang, D.M. Vaughn, G.D. Bush, A.L. Walding, A.A. Grigorian, J.S. Robinson Jr., D.K. Nakayama, Interleukin-lβ induces migration of rat arterial smooth muscle cells through a mechanism involving increased matrix metalloproteinase-2 activity, J. Surg. Res. 169 (2011) 328–336, https://doi.org/10.1016/j.jss.2009.12.010.
[24] X. Chen, J. Xu, W. Bao, H. Li, W. Wu, J. Liu, J. Pi, B. Tomlinson, P. Chan, C. Ruan, Q. Zhang, L. Zhang, H. Fan, E. Morrisey, Z. Liu, Y. Zhang, L. Lin, J. Liu, T. Zhuang, Endothelial Foxp1 regulates neointimal hyperplasia via matrix metalloproteinase-9/cyclin dependent kinase inhibitor 1B signal pathway, J. Am. Heart Assoc. 11 (2022), e026378, https://doi.org/10.1161/jaha.122.026378.
[25] K. Isoda, M. Shiigai, N. Ishigami, T. Matsuki, R. Horai, K. Nishikawa, M. Kusuhara, Y. Nishida, Y. Iwakura, F. Ohsuzu, Deficiency of interleukin-1 receptor antagonist promotes neointimal formation after injury, Circulation 108 (2003) 516–518, https://doi.org/10.1161/01.Cir.0000085567.18648.21.
[26] F. Roubille, D. Busseuil, Y. Shi, W. Nachar, T. Mihalache-Avram, M. Mecteau, M. A. Gillis, G. Brand, G. Théberge-Julien, M.R. Brodeur, A.E. Kernaleguen, M. Gombos, E. Rhéaume, J.C. Tardif, The interleukin-1β modulator gevokizumab reduces neointimal proliferation and improves reendothelialization in a rat carotid denudation model, Atherosclerosis 236 (2014) 277–285, https://doi.org/10.1016/j.atherosclerosis.2014.07.012.
[27] Z. Fan, J. Yang, C. Yang, J. Zhang, W. Cai, C. Huang, MicroRNA-24 attenuates diabetic vascular remodeling by suppressing the NLRP3/caspase-1/IL-1β signaling pathway, Int. J. Mol. Med. 45 (2020) 1534–1542, https://doi.org/10.3892/ijmm.2020.4533.
[28] Q. An, Q. Hu, B. Wang, W. Cui, F. Wu, Y. Ding, Oleanolic acid alleviates diabetic rat carotid artery injury through the inhibition of NLRP3 inflammasome signaling pathways, Mol. Med. Rep. 16 (2017) 8413–8419, https://doi.org/10.3892/mmr.2017.7594.
[29] T.C. Chen, C.K. Yen, Y.C. Lu, C.S. Shi, R.Z. Hsieh, S.F. Chang, C.N. Chen, The antagonism of 6-shogaol in high-glucose-activated NLRP3 inflammasome and consequent calcification of human artery smooth muscle cells, Cell Biosci. 10 (2020) 5, https://doi.org/10.1186/s13578-019-0372-1.